JARQ 48 (3), 307 - 316 (2014) http://www.jircas.affrc.go.jp

Field Operation of a Movable Strawberry-harvesting Robot using a Travel Platform

Shigehiko HAYASHI[1]*, Satoshi YAMAMOTO[1], Sadafumi SAITO[1], Yoshiji OCHIAI[1], Junzo KAMATA[2], Mitsutaka KURITA[2] and Kazuhiro YAMAMOTO[3]

[1] Bio-oriented Technology Research Advancement Institution, NARO (Saitama, Saitama 331-8537, Japan)
[2] Shibuya Seiki Co., Ltd. (Matsuyama, Ehime 791-8036, Japan)
[3] Ehime Research Institute of Agriculture, Forestry and Fisheries (Matsuyama, Ehime 799-2405, Japan)

Abstract

This paper describes the development of a movable strawberry-harvesting robot that can be mounted on a travel platform, along with its practical operation in a greenhouse. The harvesting robot can traverse and enter an adjacent path and picking is performed with the travel platform halted on the travel path. Machine vision is used to detect a piece of red fruit and calculate its position in the three-dimensional space, whereupon its maturity level is assessed according to an area ratio determined by classifying the whole fruit into three areas: ripe, intermediate, and unripe area fractions. Sufficiently mature fruit are picked by the end-effector by cutting the peduncle. During operational tests in a greenhouse, our machine vision algorithm to assess maturity level showed a coefficient of determination of 0.84. Setting the maturity level parameter at 70 or 80% resulted in higher shippable fruit rates than the setting of 60%, because small unripe fruit positioned in front of larger ripe fruit were successfully skipped in the former case. Our results showed that a higher shippable fruit rate could be achieved later in the harvest season, reaching 97.3% in the test in June. The successful harvesting rate and work efficiency were 54.9% and 102.5 m h^{-1}, respectively.

Discipline: Agricultural machinery
Additional key words: shippable fruit rate, successful harvesting rate, traverse function, work efficiency

Introduction

In 2011, Japanese strawberry (*Fragaria × ananassa Duch.*) production was worth JPY 157.4 trillion (MAFF), which is equivalent to the market for staple fruit such as tomatoes, cucumbers, and mandarin oranges. The high market value of strawberries is expected to help stabilize farm management. However, because strawberries are very prone to bruising, they are harvested in the early morning hours, before they lose their firmness. Strawberry harvesting is a labor-intensive task because workers need to exercise great care while handling the fruit.

Fundamental studies of a strawberry-harvesting robot are being carried out in Japan, focusing on soil culture. Several picking mechanisms have been proposed, including a rotating end-effector (Satou et al.1996), suction-type end-effector (Kondo et al. 2000), hook-type end-effector (Arima et al. 2004), and scissors-type end-effector (Cui et al. 2006). These robotic harvesters are based on a Cartesian coordinate manipulator that straddles the ridges and approaches the fruit from above, but remain laboratory prototypes for now. New approach methods from the path side (Hayashi et al. 2010) and bed side (Arima et al. 2001, Hayashi et al. 2012) have been investigated to exploit the advantages of the increasingly popular elevated-substrate culture, which has fewer obstacles around the fruit (Kondo et al. 1998). An elevated-substrate culture is widely used in Belgium, the Netherlands, and Japan (Hancock, 1999), and has recently been adopted in Korea and China (Matsumoto 2004, Wechsler 2012). In Korea, a prototype harvesting robot with a color charge-coupled device (CCD) camera and laser device has been studied (Han et al. 2012).

The Bio-oriented Technology Research Advancement Institution has launched a project to develop a strawberry-harvesting robot for an elevated-substrate culture. To

*Corresponding author: e-mail shigey@affrc.go.jp
Received 4 October 2013; accepted 9 December 2013.

address the unstructured environment found in the field, a development concept was devised for overnight operation, peduncle handling, and task-sharing with human workers. Based on this development concept, a strawberry-harvesting robot that performs autonomous harvesting by moving back-and-forth along a set of rails was developed and tested in the field (Hayashi et al. 2010). A rail system provided stable and precise travel, and previous studies on harvesting robots utilized this system (Hayashi et al. 2003, Tanigaki et al. 2008). A wheeled travelling method was also demonstrated for harvesting robots (Arima et al. 1994, Kondo et al. 1996).

Both systems utilized back-and-forth movements. In contrast, very few studies have investigated autonomous traverse movements for harvesting robots, although the conceptual design of a docking system has been proposed for a cucumber-harvesting robot (Bontsema et al. 1999, Van Henten et al. 2002) and the system requires a meticulous interlock to facilitate communication between the robot and cart.

We have devised a gantry-type travel platform that moves both along and across paths, carrying a robotic system (Hayashi et al. 2013) that exploits the advantages of a gantry system, such as accurate application and precise positioning of tools and the utilization of electric power (Monta 1998). The travel platform passes under hanging benches.

The aim of this study was to develop a movable strawberry-harvesting robot that could be mounted on a travel platform, and verify its practicability in a greenhouse. The harvesting robot has a cylindrical structure, which comprises a machine vision unit, an end-effector, and a tray storage unit. Its major advantage is that it can be configured and fine-tuned before being installed on the platform. Intercommunication between the harvesting robot and platform is carried out via digital I/O signals. An operational test was conducted in a greenhouse to determine the optimum settings for the harvesting robot and its basic performance.

Materials and methods

1. Experimental greenhouse and structure of the travel platform

Figure 1 shows an experimental greenhouse 48 m long and 6 m wide (Hayashi et al. 2013), which was built adjacent to an existing greenhouse maintained by a grower. The cultivar Amaotome was cultivated using the same forcing culture as the existing greenhouse. Six hanging benches were installed in it: three fixed-type and three rolling-type benches respectively. The width of the pathway between the rolling beds was kept adjustable to create a structural environment for robot operation. Each bench was 42.75 m long, and the test length of the harvesting robot was set at 35.25 m.

A travel platform comprising a girder frame and side-

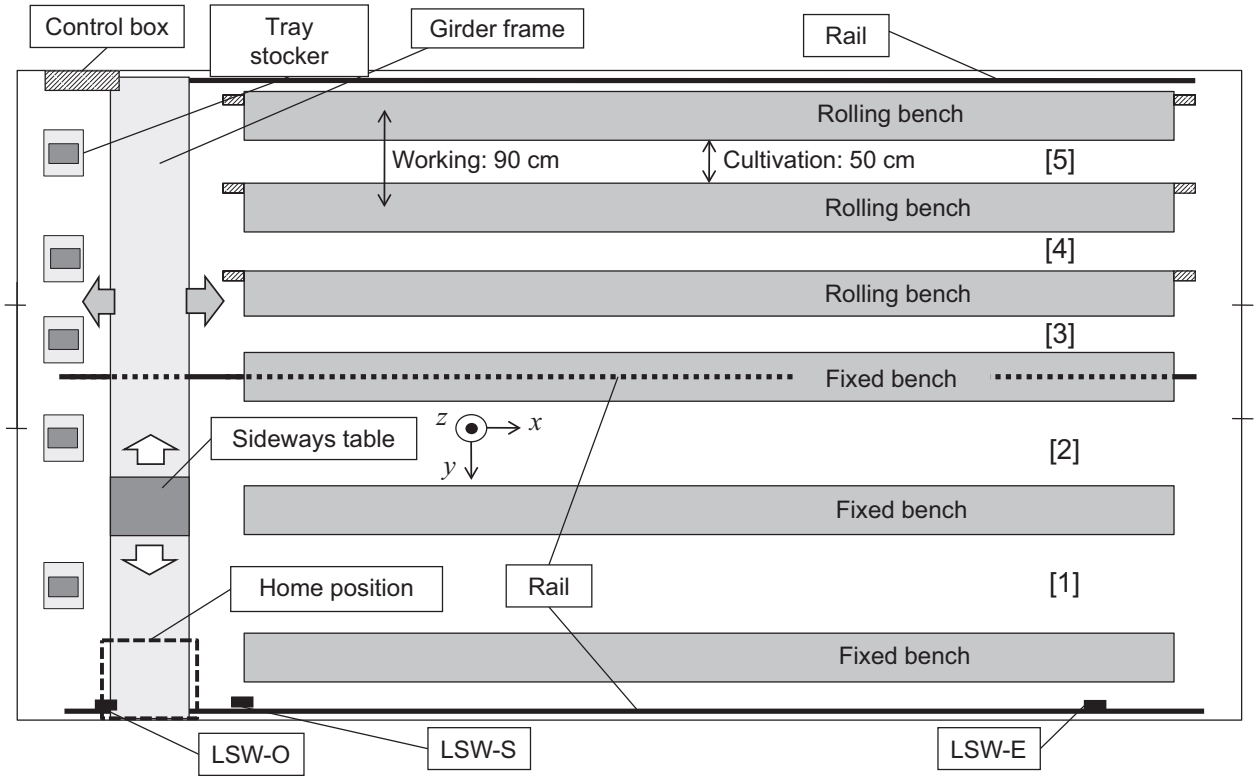

Fig. 1. Schematic diagram of experimental greenhouse for the strawberry-harvesting robot

Table 1. Specifications of the movable strawberry-harvesting robot

Item	Data
Main robot	
Size and mass	L1695 × W910 × H1935 mm, 245 kg
Machine vision	Rectangular LED light source (218 × 30 mm) Colour CCD cameras: 3
Manipulator	Type: 3DOF Cylindrical robot
End-effector	Open-close fingers with interchangeable blade 3-position finger rotation Photoelectric sensor for grasping
Tray storage	No. of trays: 4 Tray size: L535 × W255 × H80 mm
Travel platform	
Size and mass	L1200 × W5700 × H200 mm, 260 kg
Girder frame	Travel method: 210 mm step travel Max speed: 262 mm s^{-1} (set speed: 182 mm s^{-1})
Sideways table	Size: 600 × 1200 mm Max speed: 262 mm s^{-1} (set speed: 140 mm s^{-1})

ways table was assembled in the experimental greenhouse to enable the harvesting robot both to travel along the path and traverse to the next path. Table 1 lists the specifications of the travel platform and harvesting robot. The platform was 5700 mm wide and 1200 mm long. The girder moved longitudinally by 210 mm in response to signals from the harvesting robot. The travel speeds of the girder frame and sideways table during the operational tests were set at 182 and 140 mm s^{-1}, respectively.

2. Strawberry-harvesting robot

A movable strawberry-harvesting robot was developed based on the findings obtained with our previous prototype (Hayashi et al. 2010). The harvesting robot comprised a cylindrical manipulator, an end-effector, a machine vision unit, and a tray storage unit. Figure 2 shows the harvesting robot, and Table 1 lists its specifications.

(1) Manipulator

A three degrees-of-freedom (3-DOF) cylindrical manipulator was set up as part of an inverted structure in which the lower part of the manipulator was positioned upward to ensure space under the end-effector, as shown in Figures 2 and 3. The operational rotation angle and vertical and horizontal lengths were 250°, 400 mm, and 300 mm, respectively.

(2) End-effector

The end-effector comprised a gripper with two fingers for cutting the peduncle, and a reflection-type photoelectric sensor to confirm the presence of the picked fruit. An interchangeable blade and stopper were attached to one of the fingers (see Fig. 3). A cushioning material was glued to the contact side of the finger to enable it to simultaneously hold and cut the peduncle.

(3) Machine vision unit

The machine vision unit had a rectangular light-emitting diode (LED) source and three color charge-coupled device cameras. The two side cameras, each with a baseline length of 100 mm, were used to provide stereovision to determine each fruit's position within the three-dimensional (3D) space and its maturity level, while the camera in the center was used to detect the peduncle and calculate its inclination. Polarizing filters were attached to all the cameras and the LED light to diminish specular reflection. The LED light was switched on during the picking process (from

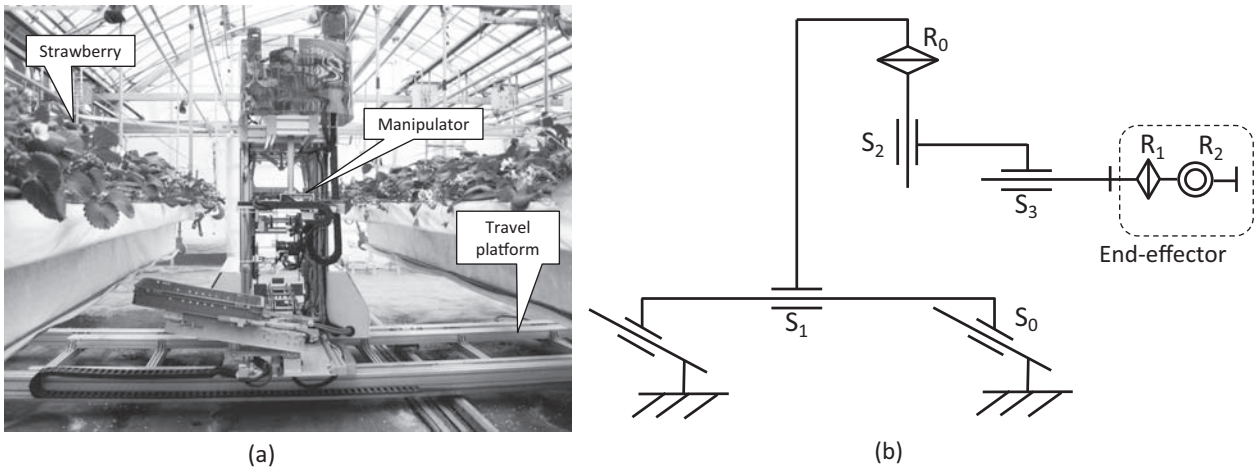

Fig. 2. Strawberry-harvesting robot

(a) general view, (b) robot structure; S_0: girder frame movement, S_1: sideways table movement, S_2: vertical slide of 400 mm, S_3: horizontal slide of 300 mm, R_0: rotation of 250°, R_1: rotation of end-effector, and R_2: tilt of end-effector.

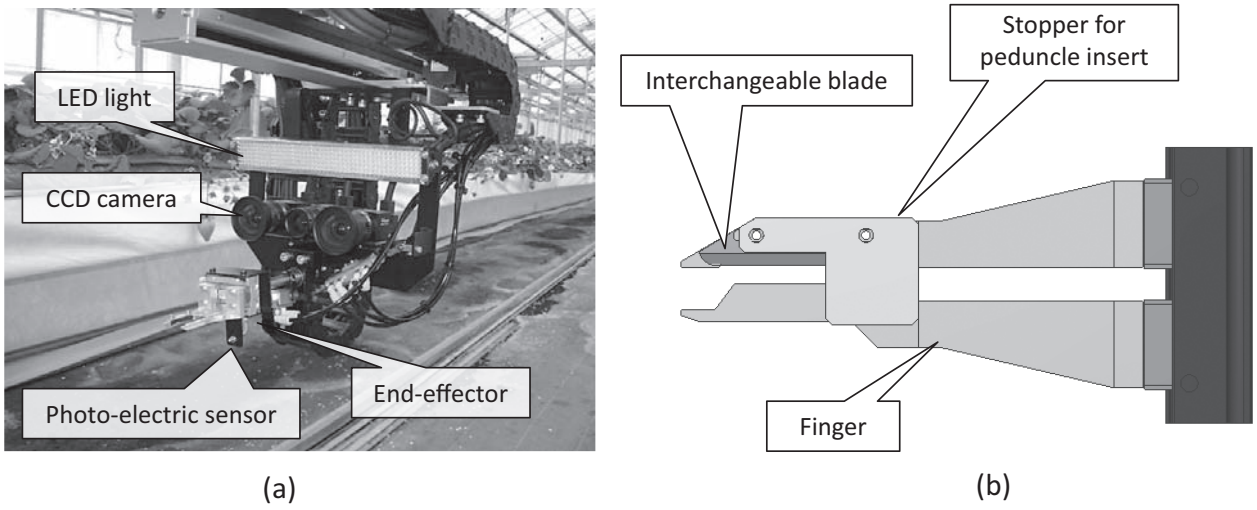

Fig. 3. Machine vision and end-effector
(a) main part and (b) end-effector.

image capture through fruit release) but not during travel. The machine vision algorithm is discussed in the section below.

(4) Tray storage unit

The tray storage was separated into two layers and configured to accommodate four trays. Each tray accommodated 84 strawberries, for a total of 336. The upper layer was used for empty trays and the lower layer for filled trays. One empty tray was withdrawn from the upper compartment and placed on a conveyor belt, which carried it into position under the end-effector. When the tray became full during the harvesting operation, the conveyor reversed direction and stacked the tray in the lowest compartment.

3. Automatic harvesting procedure using the strawberry-harvesting robot

(1) Movement in the experimental greenhouse

The strawberry-harvesting robot was linked to the rolling benches to move either along the path or sideways in the greenhouse. Communication between them was performed via digital I/O signals.

The basic movement of the strawberry-harvesting robot is illustrated in Figure 1. The sideways table, on which the harvesting robot was mounted, moved in the traverse direction, starting from the home position, and stopped at the entry point of Path [1]. Four empty trays were loaded onto the harvesting robot. The harvesting robot then moved along Path [1] in stepwise increments of 210 mm, picked the right-side strawberries in accordance with the picking procedure described in the section below, and returned after reaching the end of the path. On the way back, the harvesting robot picked the left-side strawberries. When the picking task for Path [1] was finished, the harvesting robot discharged the filled trays to the tray stocker at the entry point and returned to its home position. If all four trays became full, the harvesting robot halted the picking task and automatically proceeded to the entry point to discharge the filled trays. After this round-trip movement, the platform repeated the same process for Paths [2], [3], [4], or [5], if they were selected.

(2) Picking procedure

After the travel platform halted, the picking task was performed by following the procedure shown in Figure 4. Our procedure employed the machine vision algorithm used in a previous study (Hayashi et al. 2010), which segments the fruit's area using hue-saturation-intensity (HSI) images converted from red-green-blue images. However, the threshold values were changed and adjusted in the field to adapt to the reflection sheets fitted between the bench and fruit to promote the coloring of the back side of the fruit.

Moreover, this study integrated a new method for classifying the whole fruit area into three area fractions to assess its maturity level. The ripe area fraction (*Rr*) was detected as the region satisfying the following color conditions, as shown in Figure 5-(c):

$$\begin{cases} 1 \le H \le 18 \\ 100 \le S \le 180 \\ 1 \le I \le 255 \end{cases} \quad (1)$$

The intermediate area fraction (*Ir*) was detected as the region satisfying the following color conditions, as shown in Figure 5-(d):

$$\begin{cases} 14 \le H \le 30 \\ 40 \le S \le 140 \\ 1 \le I \le 255 \end{cases} \quad (2)$$

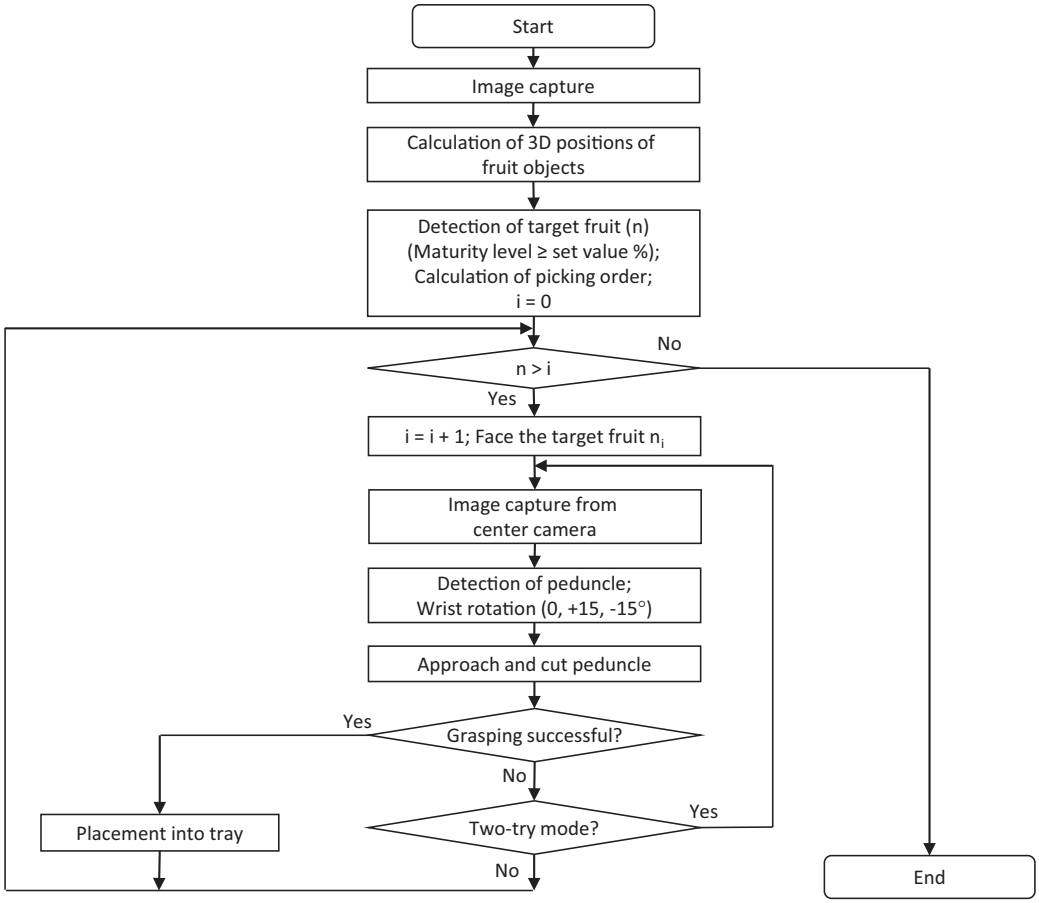

Fig. 4. Operational flowchart for the strawberry-harvesting robot

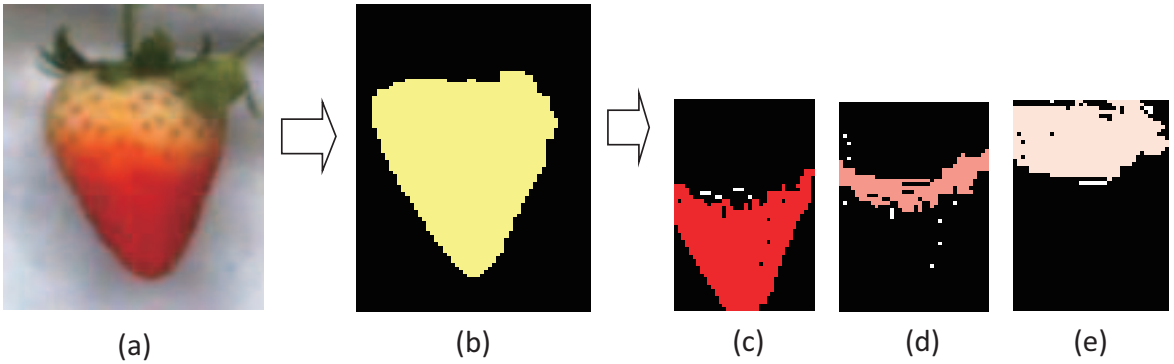

Fig. 5. Image processing for the maturity level assessment
(a) target red fruit, (b) whole fruit area, (c) ripe area, (d) intermediate area, and (e) unripe area.

The unripe area fraction (*Ur*) was detected as the region satisfying the following color condition, as shown in Figure 5-(e):

$$\begin{cases} 13 \le H \le 180 \\ 40 \le S \le 120 \\ 1 \le I \le 255 \end{cases} \quad (3)$$

The maturity level (*Mv*) was then computed using Equation (4):

$$Mv = \frac{Rr + Ir \times w}{Rr + Ir \times Ur} \times 100 \quad (4)$$

where *w* is the weighted value, which varies according to the cultivar, but was set at 0.05 for Amaotome in this study. Sufficiently mature fruit, whose maturity level (*Mv*) is equal to or exceeds the selected value, are recognized as target fruit and picking attempts are made in order of distance to

the target fruit.

The machine vision unit and end-effector face the first target fruit. The end-effector then moves to a position approximately 275 mm in front of the target fruit. Here, the center camera captures an image, and the area of the target fruit is extracted for peduncle detection.

The region of interest (ROI) for searching for the peduncle is set at 20 pixels above the region of the target fruit. The ROI is 15 pixels in height, and the pixel width is equal to the breadth of the fruit. Potential objects are detected using HSI images, and the candidate object closest to the top of the target fruit is selected as the peduncle. The angle of the line connecting the centroid of the peduncle and the top of the target fruit in relation to the vertical is defined as the inclination of the peduncle (*Ip*), as shown in Figure 6. After this image processing, the end-effector wrist rotates to one of three positions, 0, +15, or –15°, corresponding to *Ip*; but the end-effector remains vertical if the machine vision unit is unable to detect the peduncle.

The gripper fingers approach the detected peduncle, then grasp and cut it simultaneously. The manipulator returns to its original position and checks whether the fruit has been grasped with the reflection-type photoelectric sensor attached on the end-effector. If the end-effector holds the fruit correctly, the end-effector proceeds to tilt and place it in the tray. If the end-effector fails to cut the peduncle, the harvesting robot proceeds according to the selected picking mode: in the one-try mode, the robot looks for the next fruit, while in two-try mode, the robot retries, starting from the peduncle detection step, although there is no third try. This picking task is attempted for all the target fruit detected by the stereovision.

4. Operational testing in an experimental greenhouse

(1) Maturity level assessment (Test 1)

The maturity levels as assessed by the machine vision and a human worker were compared using Amaotome. A sample fruit was placed in front of the camera, and the maturity level assessment process was executed. The maturity levels fell within the range 50–100%, in increments of 10%. Each level had five samples, resulting in a total of 30 strawberries.

(2) Basic harvest performance (Test 2)

The successful harvesting rate (*SHR*) was measured to derive the basic performance of the strawberry-harvesting robot using Amaotome. A test length of 35.25 m was set on both sides of a pathway. The target mature fruit, with maturity of 80% or more, were marked and counted before the robot operation. The harvesting robot then executed autonomous harvesting under fixed parameters of a maturity level of 80% and the two-try mode. After counting the mature fruit successfully picked, the *SHR* was calculated using Equation (5):

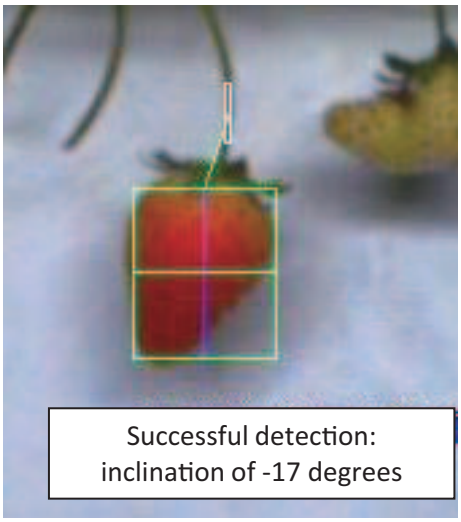

Fig. 6. Image processing for peduncle detection

$$SHR = Ns/Nt \times 100 \quad (5)$$

where *Ns* is the number of successfully harvested mature strawberries, and *Nt* is the number of target mature strawberries marked before the test.

(3) Parameter settings of the harvesting robot (Test 3)

In Test 2, the basic harvesting performance was derived based on target mature samples with a maturity level of 80% or more. The immature fruit picked were therefore classified as failed attempts. However, it was observed during the field operation of the robot that the grower shipped red immature fruit slightly before maturation, which suggests that the shipment standard has some tolerance in the maturity level: for instance, in cases where a human picks an immature fruit by mistake, it is sent to the market, if undamaged.

This study employed a new criterion for evaluating the robot performance: the shippable fruit rate (*SFR*). The fruit harvested by the robot comprised shippable and non-shippable fruit: the former included fruit whose maturity level was approximately 60% or more, with no bruises or abrasions; conversely, non-shippable fruit included green immature fruit, small fruit, and damaged fruit. Therefore, the *SFR* was defined using Equation (6):

$$SFR = Fs/Ft \times 100 \quad (6)$$

where *Fs* represents the pieces of shippable fruit, and *Ft* represents the total pieces of fruit harvested by the robot.

The harvesting robot had several parameter settings, which significantly affected the harvesting performance. In Test 3, the influence of the parameter settings was evaluated using *SFR*. The harvesting robot executed autonomous picking movements along both sides of a pathway under several parameter settings for the maturity level and pick-try

Table 2. Experimental conditions of parameter settings in Test-3 and results

Trial	Harvest day	Maturity level setting	Try mode	Shippable fruits	Non-shippable fruit *	SFR (%)	Test length (m)	Executional time (s)	Harvested fruit per hour (fruit h^{-1})	Work efficiency (m h^{-1})
1	11-Apr	60%	Two-try	180	177 (0)	50.4	63.75	4056	159.8	56.6
2	11-Apr	70%	Two-try	214	91 (1)	70.2	52.25	3515	219.2	53.5
3	11-Apr	80%	Two-try	174	52 (0)	77.0	70.50	3596	174.2	70.6
4	15-May	80%	One-try	36	8 (0)	81.8	70.50	1763	73.5	144.0
5	15-May	80%	One-try	33	3 (0)	91.7	70.50	1710	69.5	148.4
6	15-May	80%	Two-try	25	2 (0)	92.6	70.50	1638	55.0	155.0
7	5-Jun	70%	Two-try	127	14 (1)	90.1	70.50	2847	160.6	89.2
8	5-Jun	80%	One-try	53	1 (0)	98.1	70.50	1870	102.0	135.7
9	5-Jun	80%	Two-try	73	2 (0)	97.3	70.50	2232	117.7	113.7

*: A number in parenthesis shows damaged fruit.

mode. The maturity level of the machine vision algorithm was set at 60, 70, or 80%, and the pick-try mode was set as one- or two-try. Nine trials were conducted and their parameter settings are listed in Table 2.

After each trial, the fruit harvested by the robot was classified into shippable and non-shippable fruit by the grower. The elapsed execution time for each operation was also measured to calculate the work efficiency.

Results and discussion

1. Maturity level assessment (Test 1)

Figure 7 shows the results of a maturity level assessment using the machine vision in Test 1. A coefficient of determination of 0.84 indicated the potential usefulness of our algorithm, which used three classifications: red, intermediate, and unripe area fractions. However, the machine vision assessment tended to show a wider range of scattering at maturity levels of 50–60% than at 90–100%. At each human-assessed maturity level, the maturity level ranges judged by the machine vision overlapped, showing that machine vision, using the current method, is still unable to thoroughly distinguish the maturity level as precisely as human workers.

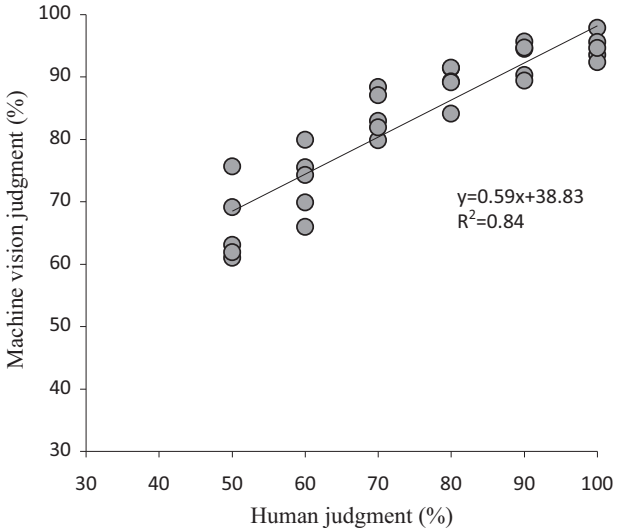

Fig. 7. Comparison of maturity level assessments between human workers and machine vision

2. Successful harvesting rate (Test 2)

In Test 2, the harvesting robot was successfully able to pick 73 of the 133 mature pieces of fruit, giving an *SHR* of 54.9%. This value of 73 included three pieces of fruit that were picked successfully on the second attempt. Moreover, two immature strawberries were picked simultaneously with a mature strawberry, giving a total weight of 9 g (average: 4.5 g). Of the 60 strawberries that the robot failed to pick, 57 were undetected as target fruit because they were eclipsed by other fruit. In the other three cases, the robot failed to cut the peduncle using the end-effector due to peduncle detection errors.

Because our machine vision system projects the fruit in a 3D space on an image frame, the system lacks spatial perception, namely, the distance information disappears. Consequently, further studies would need a strategy for spatial perception based on the 3D vision techniques employed for other crops (Noordam et al. 2005, Rath & Kawollek 2009). At the same time, there is a need for a new approach mechanism for picking hidden fruit that does not damage adjacent fruit.

3. Parameter settings of the harvesting robot (Test 3)

(1) Effects of parameter settings for harvesting robot on fruit shipment

Table 2 lists the *SFR* results at various parameter settings in Test 3. A comparison of trials 1–3 to investigate the effect of the parameter setting for the maturity level showed

a tendency for *SFR* to rise with increasing maturity level setting, as shown in Figure 8. However, it leveled off between 70 and 80%. It was inferred that the low *SFR* with a maturity level setting of 60% was due to the poor maturity level assessment by the machine vision: for instance, immature fruit partially eclipsing red fruit was treated as target fruit in the image frame and accordingly — and incorrectly — picked. However, at settings of 70–80%, these immature fruit were rejected, due to their large green portions. This result suggests that a 60% maturity level is an inappropriate setting for practical use of the harvesting robot.

When comparing trials 4–6 and 7–8 in Test 3 to investigate the effect of the try-mode parameter setting, no statistical significance between the one- and two-try modes was found in either May or June, which suggests that a second attempt did not contribute to improved picking success because the positional error when imaging a peduncle could not be corrected by detecting it a second time. Adopting a different viewpoint would effectively counter this problem, but the manipulator would need an additional DOF to slide the end-effector, further complicating the mechanism.

Of the non-shippable fruit in Test 3, in trials 2 and 7, two strawberries were observed to have been damaged by being stabbed with the fingers due to proximity to the target fruit peduncle. To prevent this, the machine vision algorithm needs an additional constraint in the process for detecting a peduncle.

(2) Effect of the harvest season

The clustered fruit setting form changes considerably according to the season and inflorescence, which means these factors will affect the robot harvest performance. A comparison of trials 3, 6, and 9 in Test 3 to verify the effect of the harvest season on *SFR* revealed that a later harvest season resulted in a higher *SFR*, which rose to 97.3% in the test in June, as shown in Figure 9. This was likely due to the decreasing overlap between the target fruit and immature fruit later in the season. For a one-season-bearing cultivar such as Amaotome, fruit cluster emergence would have been restrained as summer approached; consequently, the overlap lessened.

(3) Work efficiency

During trials 2–9 in Test 3 (from which trial 1 was excluded due to an inappropriate setting), the work efficiency, defined as the operational distance travelled per hour, was 53.5–155.0 m h^{-1} (average: 102.5 m h^{-1}) and varied in proportion to the quantity of the harvested fruit. This relationship is shown in Figure 10. It can be seen that the operational length shows an almost inversely proportional relationship to the quantity of harvested fruit.

Our investigation revealed that the distance travelled per hour was 242–1638 m h^{-1} (average: 938 m h^{-1}) for a single worker picking the same area, which meant a considerable difference between the work efficiencies of the harvesting robot and the human workers, in addition to the low *SHR* of the harvesting robot. Several further studies could be conducted to cope with this difference, the most direct of which would be to accelerate each motion of the harvesting robot. A second method would involve increasing the operational hours per day. Although the developed robot works basically only at night, if lighting conditions similar to nighttime were created by shielding the sun during the daytime, the work efficiency gap between human

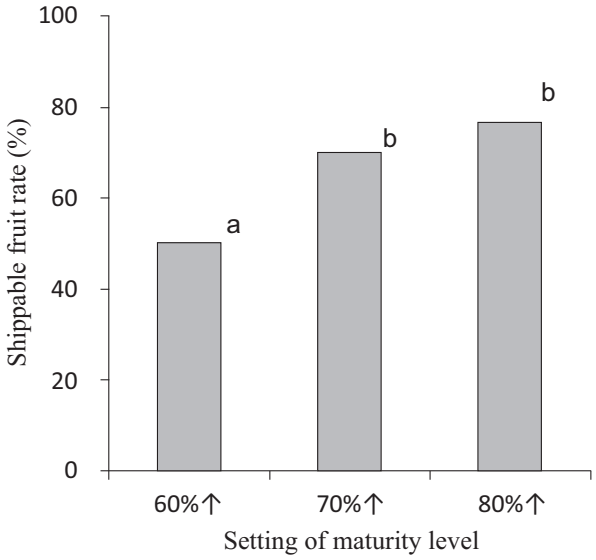

Fig. 8. Relationship between set maturity level and shippable fruit rate (*SFR*)
Letters at the top right of bars indicate that *SFR*s with the same letter do not differ significantly at a 5% level according to the χ^2 test.

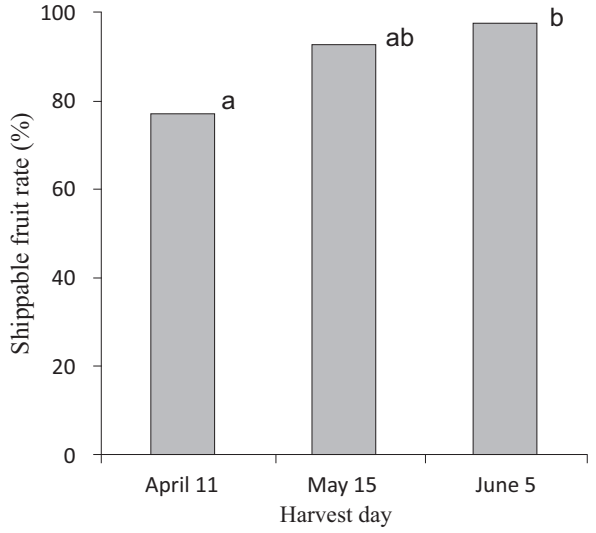

Fig. 9. Relationship between the harvest season and SFR
Letters at the top right of bars indicate that *SFR*s with the same letter do not differ significantly at a 5% level according to the χ^2 test.

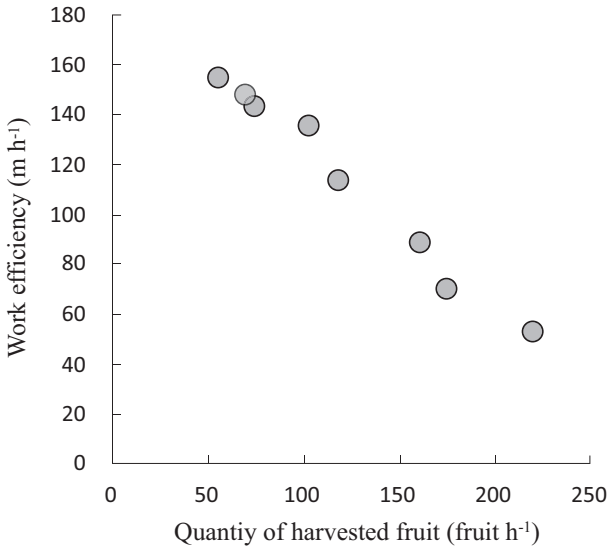

Fig. 10. Relationship between the quantity of harvested fruit (fruit h^{-1}) and work efficiency (m h^{-1})

workers and robots could be narrowed. A third method might be to abandon stepwise movement during path travel. The harvesting robot could reach mature fruit more rapidly by adding a function to search for mature fruit while travelling, or by utilizing fruit images recorded several days beforehand to forecast a suitable picking day.

Conclusions

Prompted by the need for labor-saving in strawberry production, a movable strawberry-harvesting robot that can be mounted on a travel platform was developed and operated practically in a greenhouse. The harvesting robot and travel platform are modular system units that can be individually configured and fine-tuned. The harvesting robot comprised a 3-DOF cylindrical manipulator, end-effector, machine vision unit, and tray storage unit. The harvesting robot, combined with the travel platform, demonstrated the potential for autonomous harvesting in a two-dimensional area in a greenhouse.

Picking was performed with the travel platform halted along the path of travel. Machine vision detected red pieces of fruit and calculated their maturity levels and positions in 3D space from the images. The process for assessing the maturity level classified the target fruit area into three types: ripe, intermediate, and unripe, using HSI images. If the fruit was sufficiently mature, the machine vision searched for the peduncle and estimated its inclination. The end-effector wrist then rotated corresponding to the inclination, and picked the target fruit.

The machine vision algorithm to assess maturity level showed a high coefficient of determination of 0.84 in comparison with human judgment (Test 1). However, the algorithm tended to show wide scattering in maturity level assessments of 50–60% as judged by humans, which mutually overlapped. This revealed the inability of machine vision, at least using the current method, to distinguish the maturity level based on color as effectively as human judgment.

The basic harvesting performance was shown by an *SHR* of 54.9% with a maturity level parameter setting of 80% in the two-try mode (Test 2).

In operational testing in a greenhouse (Test 3), setting the maturity level parameter at 70 or 80% resulted in a higher *SFR* than that found with the 60% setting, which means these settings appear suitable for practical use. However, no clear differences emerged between the one- and two-try modes. It was also shown that a higher *SFR* could be obtained later in the harvest season; a value of 97.3% was obtained in the test in June. The work efficiency of the harvesting robot, defined as the operational distance travelled per hour, was 102.5 m h^{-1}.

References

Arima, S. et al. (1994) Studies on cucumber harvesting robot (part 1). *J. Jpn. Soc. Agric. Machin.*, **56(1)**, 55-64 [In Japanese with English abstract].

Arima, S. et al. (2001) Harvesting robot for strawberry grown on table top culture (part 1). *J. Sci. High Tech. Agric.*, **13**, 159-166 [In Japanese with English abstract].

Arima, S. et al. (2004) Multi-operation robot for strawberry cultivation. *Proceedings of Robomec2004*, Nagoya, Japan, 2P2-L2-14 [In Japanese with English abstract].

Bontsema, J. et al. (1999) Automatic harvesting of vegetable fruits. *Proceed. BRAIN Int. Symp.*, Omiya, Japan, 44-51.

Cui, Y. et al. (2006) Study on strawberry harvesting robot using machine vision for strawberry grown on annual hill top (part 1). *J. Jpn. Soc. Agric. Machin.*, **68(6)**, 59-67 [In Japanese with English abstract].

Han, K. S. et al. (2012) Strawberry Harvesting Robot for Bench-type Cultivation. *J. Biosyst. Eng.*, **37**, 65-74.

Hancock, J. (1999) Tunnels and forcing systems, Strawberries. *CABI Publishing*, NY, USA, 122-124.

Hayashi, S. et al. (2002) Robotic harvesting system for eggplants. *JARQ*, **36**, 163-168.

Hayashi, S. et al. (2003) Robotic Harvesting System for Eggplants Trained in V-Shape (part 1). *J. Sci. High Tech. Agric.*, **15**, 205-210 [In Japanese with English abstract].

Hayashi, S. et al. (2010) Evaluation of a strawberry-harvesting robot in a field test. *Biosyst. Eng.*, **105**, 160-171.

Hayashi, S. et al. (2012) Study on an inside-approach harvesting robot for picking strawberries. *J. Jpn. Soc. Agric. Machin.*, **74**, 325-333 [In Japanese with English abstract].

Hayashi, S. et al. (2013) Structural environment suited to the operation of a strawberry-harvesting robot mounted on a travelling platform. *Eng. Agric. Environ. Food*, **64**, 34-40.

Kondo, N. et al. (1996) Visual Feedback Guided Robotic Cherry Tomato Harvesting. *Trans. ASAE*, **39**, 2331-2338.

Kondo, N. et al. (1998) Strawberry-harvesting robot. *In* Robotics for bioproduction systems, eds. Kondo N. & Ting K. C.

ASAE Publication, MI, USA, 212-213.
Kondo, N. et al. (2000) Harvesting robot for strawberry grown on annual hill top (part 1). *J. Sci. High Tech. Agric.*, **12**, 23-29 [In Japanese with English abstract].
MAFF: Statistics on Agricultural Income Produced. http://www.maff.go.jp/j/tokei/kouhyou/nougyou_sansyutu/index.html.
Matsumoto, T. (2004) Situation of strawberry production in Korea. *Greenhouse Hortic.*, **126**, 59-63 [In Japanese].
Monta, M. (1998) Gantry system. *In* Robotics for bioproduction systems, eds. Kondo N. & Ting K.C. ASAE Publication, MI, USA. 141-144.
Noordam, J. C. et al. (2005) Automated Rose Cutting in Greenhouses with 3D Vision and Robotics. *Acta Hortic.*, **691**, 885-892.
Rath, T. & Kawollek, M. (2009) Robotic harvesting of Gerbera *Jamesonii* based on detection and three-dimensional modeling of cut flower pedicels. *Comput. Electron. Agric.*, **66**, 85-92.
Satou, T. et al. (1996) Development of a strawberry-harvesting robot. *Proceedings of the 55th Annual Meeting of JSAM*, Hokkaido, Japan, 243-244 [In Japanese].
Tanigaki, K. et al. (2008) Cherry-harvesting robot, *Comput. Electron. Agric.*, **63**, 65-72.
Van Henten, E. J. et al. (2002) An Autonomous Robot for harvesting cucumbers in greenhouses. *Auton. Robot*, **13**, 241-258.
Wechsler, D. (2012) Gathering in China. *Am./West. Fruit Grow.*, **132**, 18-20.